PHYSICAL REVIEW B **70**, 100201(R) (2004)

Compatibility factor of segmented thermoelectric generators based on quasicrystalline alloys

Enrique Maciá*
Departamento de Fisica de Materiales, Facultad CC. Fisicas, Universidad Complutense de Madrid, E-28040, Madrid, Spain
(Received 26 May 2004; published 13 September 2004)

In this work we present a prospective study on the possible use of certain quasicrystalline alloys in order to improve the efficiency of segmented thermoelectric generators. To this end, we obtain a closed analytical expression for their compatibility factor [G. J. Snyder and T. S. Ursell, Phys. Rev. Lett. **91**, 148301 (2003)]. By comparing our analytical results with available experimental data we conclude that a promising high temperature material, compatible with benchmark thermoelectric materials, can be found among AlPdMn based icosahedral quasicrystals.

DOI: 10.1103/PhysRevB.70.100201 PACS number(s): 61.44.Br, 71.20.−b, 72.15.Jf, 85.80.Fi

The efficiency of a thermoelectric device depends on the transport properties of the constituent materials and the temperature difference between the hot and cold sides, which sets its Carnot upper limit. Evaluation of new materials for thermoelectric applications is usually made in terms of the dimensionless figure of merit,

$$ZT \equiv \frac{\sigma\alpha^2 T}{\kappa_e + \kappa_{ph}}, \tag{1}$$

where T is the temperature, $\sigma(T)$ is the electrical conductivity, $\alpha(T)$ is the Seebeck coefficient, $\kappa_e(T)$ is the charge carrier contribution to the thermal conductivity, and $\kappa_{ph}(T)$ is the lattice contribution to the thermal conductivity. When considering segmented devices one should also consider the *compatibility factor* defined by[1]

$$s = \frac{\sqrt{1+ZT}-1}{\alpha T}, \tag{2}$$

since materials with dissimilar s vales cannot be efficiently combined in that case. The thermoelectric compatibility of several materials of current technological interest has been recently reviewed, concluding that a semimetallic material with high p-type thermopower is required for development of segmented generators.[2]

In the last few years it has been progressively realized that quasicrystals (QCs) deserve some attention as potential thermoelectric materials (TEMs), since they naturally fulfill the Slack's requirements for a material belonging to the "electronic crystal/phonon glass" class.[3–7] Quite interestingly, relatively high, positive thermopower values (+100 −120 μV K^{-1}) have been reported for representatives of the icosahedral AlPdMn and AlPdRe families in the temperature range 300–600 K.[8–10] The main aim of this paper is to show that, by a judicious choice of sample's stoichiometry,[11] suitable candidates for a high temperature material, compatible with PbTe, $(AgSbTe_2)_{0.15}(GeTe)_{0.85}$ (TAGS) or skutterudites, may be found among the AlPd(Re,Mn) quasicrystalline alloys.

To this end, let us start by briefly summarizing some relevant experimental data. In Tables I and II we list the figure of merit and compatibility factors of different QCs as reported in the literature. At room temperature we observe that the largest s values are comparable to those observed in usual TEMs, like Bi_2Te_3 or SiGe ($s \simeq 1$ V^{-1}).[2] At higher temperatures the most promising QC is *i*-AlPdMn, which exhibits an s factor larger than those reported for SiGe ($s \simeq 1$ V^{-1}) and PbTe ($s \simeq 1.2$ V^{-1}), and approaches that of TAGS ($s \simeq 2.7$ V^{-1}) at $T = 550$ K.[2] On the other hand, the s factor corresponding to AlPdRe samples is larger at room temperature (where it exhibits a lower ZT value) than it is at higher temperatures (albeit it exhibits a larger ZT value). This result highlights the importance of properly balancing the ZT and s contributions in designing optimized devices.

In order to gain some theoretical insight into this question we obtain a closed analytical expression for the compatibility factor within the Kubo-Greenwood framework.[15] The central information quantities are the kinetic coefficients,

$$\mathcal{L}_{ij}(T) = (-1)^{i+j}\int \sigma(E)(E-\mu)^{i+j-2}\left(-\frac{\partial f}{\partial E}\right)dE, \tag{3}$$

where $f(E,\mu,T)$ is the Fermi-Dirac distribution function. In this formulation all the microscopic details of the system are included in the $\sigma(E)$ function. As a first approximation we will assume $\mu(T) \approx E_F$. Then, by expressing (3) in terms of the scaled variable $x \equiv (E-\mu)/k_BT$, the transport coefficients can be written as[6,16]

$$\sigma(T) = \frac{J_0}{4}, \tag{4}$$

$$\alpha(T) = -\frac{k_B}{|e|}\frac{J_1}{J_0}, \tag{5}$$

$$\kappa_e(T) = \frac{k_B^2 T}{4e^2}\left(J_2 - \frac{J_1^2}{J_0}\right), \tag{6}$$

where we have introduced the reduced kinetic coefficients,

$$J_n(T) = \int x^n \sigma(x)\,\mathrm{sech}^2(x/2)dx. \tag{7}$$

In previous works[16–18] it has been shown that the experimental $\sigma(T)$ and $S(T)$ curves of several QCs can be consistently described in terms of the two-Lorentzian spectral conductivity function,[19,20]

TABLE I. Room temperature thermopower, figure of merit, and compatibility factors for samples belonging to different quasicrystalline families.

Sample	Ref.	α (μV K^{-1})	ZT	s (V^{-1})
AlCuFe	12	+44	0.01	0.38
AlCuRuSi	12	+50	0.02	0.66
CdYb	13	+16	0.01	1.04
AlPdRe	14	+95	0.07	1.21
AlPdMn	5	+85	0.08	1.54

$$\sigma(E) = \frac{B}{\pi}\left[\frac{\gamma_1}{(E-\delta_1)^2+\gamma_1^2} + A\frac{\gamma_2}{(E-\delta_2)^2+\gamma_2^2}\right]^{-1}, \quad (8)$$

where B is a scale factor expressed in Ω^{-1} cm^{-1} eV^{-1} units, and the Lorentzian peaks are characterized by their height, $(\pi\gamma_i)^{-1}$, and their position, δ_i, with reference to the Fermi level. The overall behavior of this curve agrees well with the experimental results obtained from tunneling and point contact spectroscopy measurements, where the presence of a dip feature of small width (20–60 meV, narrow Lorentzian), superimposed onto a broad (0.5–1 eV, broad Lorentzian), asymmetric pseudogap has been reported.[21–25] The relative importance of each spectral feature in the overall electronic structure is tuned through the weight factor A in Eq. (8). Making use of Eq. (8) into Eq. (7) we get[16]

$$\begin{pmatrix} J_0 \\ J_1 \\ J_2 \end{pmatrix} = 4\sigma_0 \begin{pmatrix} 1 & 0 & \xi_2 & 0 & \xi_4 & 0 & j_0 \\ 0 & 2\xi_1 & 0 & 2\xi_3 & 0 & 2j_1 & 0 \\ \frac{\pi^2}{3} & 0 & \frac{\pi^2}{3}\frac{21}{5}\xi_2 & 0 & \frac{\pi^2}{3}j_2 & 0 & 0 \end{pmatrix} \times \begin{pmatrix} 1 \\ \frac{bT}{k_B} \\ bT^2 \\ \frac{b^2T^3}{k_B} \\ b^2T^4 \\ \frac{b^3T^5}{k_B} \\ b^3T^6 \end{pmatrix}, \quad (9)$$

where $\sigma_0 = \sigma(T \to 0)$ is the residual electrical conductivity, and $b \equiv e^2\mathcal{L}_0$, where $\mathcal{L}_0 = \pi^2 k_B^2/3e^2 = 2.44 \times 10^{-8}$ V^2 K^{-2} is the Lorenz number The phenomenological coefficients ξ_i, as well as the parametric functions $j_i = j_i(\xi_3, \xi_4)$, are directly related to the sample's electronic structure. In particular, we have[17]

$$\xi_1 = \frac{1}{2}\left(\frac{d \ln \sigma(E)}{dE}\right)_{E_F}, \quad (10)$$

so that, according to Mott's expression, ξ_1 can be derived from the low temperature slope, a, of the experimental $\alpha(T)$ curve as[18]

TABLE II. High temperature thermopower, figure of merit, and compatibility factors for samples belonging to the AlPd(Mn,Re) icosahedral family. T^* denotes the temperature maximizing the figure of merit.

Sample	Ref.	T^*	α^* (μV K^{-1})	ZT^*	s^* (V^{-1})
AlPdMn	5	550	+105	0.25	2.04
AlPdReRu	10	700	+100	0.15	1.03
AlPdRe	9	660	+90	0.11	0.90

$$\xi_1^{\exp} \simeq -20.5\, a[\mu\text{V K}^{-2}]\ (\text{eV})^{-1}. \quad (11)$$

Making use of Eq. (9) into Eqs. (4)–(6) and Eqs. (1) and (2) we get

$$s = -Q\left[\sqrt{\frac{1}{1-R}} - 1\right] \quad \text{V}^{-1}, \quad (12)$$

where

$$Q(T) = \frac{P_0}{2bT^2P_1}, \quad (13)$$

$$R(T) = \frac{2P_1}{Q(P_2+\Psi)}, \quad (14)$$

$\psi(T) \equiv \kappa_{ph}(T)/\sigma_0\mathcal{L}_0T$, and we have introduced the polynomials

$$P_0(T) \equiv 1 + (2\xi_1^2 + \Omega)y + \xi_4 y^2 + j_0 y^3, \quad (15)$$

$$P_1(T) \equiv \xi_1 + \xi_3 y + j_1 y^2, \quad (16)$$

$$P_2(T) \equiv 1 + \frac{21}{5}(2\xi_1^2 + \Omega)y + j_2 y^2, \quad (17)$$

where

$$\Omega \equiv \frac{1}{2}\left(\frac{d^2 \ln \sigma(E)}{dE^2}\right)_{E_F}, \quad (18)$$

measures the curvature of $\sigma(E)$ at the Fermi level.[17] At a given temperature Eq. (12) can be regarded as a parametric function of the different phenomenological coefficients, i.e., $s(\xi_i)$. We note that the thermal conductivity of QCs is mainly determined by the lattice contribution rather than the charge carriers in the considered temperature range.[26] Therefore, we can confidently assume $\kappa_{ph} \simeq k$ in Eq. (14), where $\kappa \equiv \kappa_e + \kappa_{ph}$ is the experimentally measured total thermal conductivity.

In Fig. 1 we compare the room temperature compatibility factors of i-AlPdRe [$\kappa = 0.7$ Wm^{-1} K^{-1},[9] $\sigma_0 = 30$ (Ω cm)$^{-1}$ (Ref.[27]) and i-AlPdMn [$\kappa = 1.6$ Wm^{-1} K^{-1}, $\sigma_0 = 740$ (Ω cm)$^{-1}$, (Ref. [5]) as a function of ξ_1. These curves are derived from Eqs. (12)–(17) with $\Omega = 400$ (eV)$^{-2}$ (Ref. 17); $\xi_3 = -2910$ (eV)$^{-3}$, $\xi_4 = 17000$ (eV)$^{-4}$, $j_0 = 10^5$ (eV)$^{-4}$, $j_1 = 130000$ (eV)$^{-4}$, and $j_2 = -30000$ (eV)$^{-4}$.[11] In order to check the feasibility of the adopted model parameters we have determined the value of the ξ_1 coefficient corresponding to the

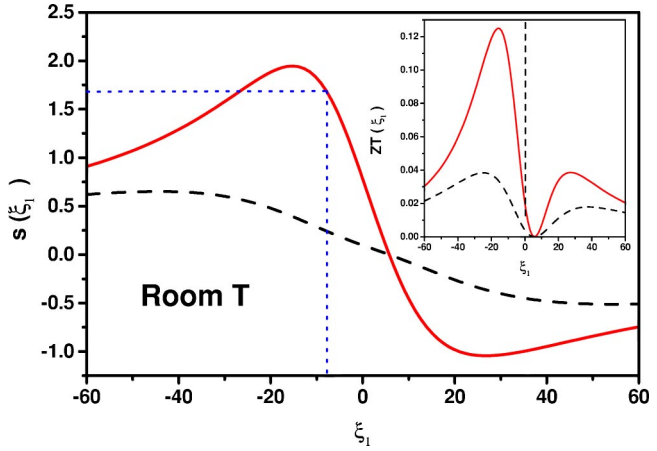

FIG. 1. (Color online) Room temperature dependence of the compatibility factor (main frame) and the thermo-electric figure of merit (inset) as a function of the phenomenological coefficient ξ_1 for *i*-AlPdRe (dashed line), and *i*-AlPdMn (solid line).

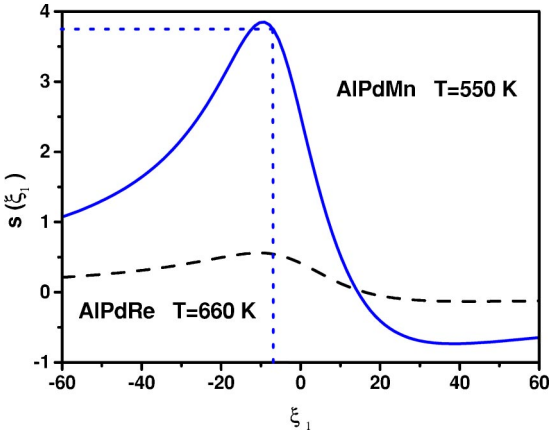

FIG. 2. (Color online) Dependence of the compatibility factor as a function of the phenomenological coefficient ξ_1 for *i*-AlPdRe with $\kappa=1.2$ Wm^{-1} K^{-1} at $T=660$ K (dashed line);[9] and AlPdMn with $\kappa=2.1$ Wm^{-1} K^{-1} at $T=550$ K (solid line) (Ref. 5).

i-AlPdMn sample. Making use of the low temperature thermopower data reported in Ref. 5 into Eq. (11) we get $\xi_1^{\exp}=-6.49$ (eV)$^{-1}$. By plugging this value in our analytical expressions we obtain $s(\xi_1^{\exp})=1.57$ V^{-1} (the dotted line in Fig. 1) and $ZT(\xi_1^{\exp})=0.080$, in excellent agreement with the experimental values listed in Table I.

The difference between the AlPdRe and AlPdMn $s(\xi_1)$ curves is due to the significant difference between their respective residual conductivities, determining the Ψ value in Eq. (14). In the inset of Fig. 1 we plot the corresponding $ZT(\xi_1)$ curves, which exhibit a deep minimum, flanked by two maxima. According to Eq. (2), both ZT and s vanish at $\xi_1^0=+5.76$ (eV)$^{-1}$. Consequently, QCs can exhibit *p*-type ($\xi_1<\xi_1^0$) or *n*-type ($\xi_1>\xi_1^0$) thermopowers depending on the ξ_1 value which, according to Eq. (10), is very sensitive to the sample's electronic structure near E_F. In fact, the electronic structure of QCs is characterized by the presence of a narrow pseudogap in the density of states close to the Fermi level. Thus, when E_F is located at the left (right) of the pseudogap's minimum ξ_1 takes negative (positive) values, and its magnitude is directly related to the $\sigma(E)$ slope. Therefore, the ξ_1 value can be controlled by changing the sample stoichiometry, hence shifting E_F in a scale of a few meV. In this way, we can confidently expect that larger values of the room temperature compatibility factor, close to $s=2.0$ V^{-1} may be attained in AlPdMn QCs with $\xi_1\simeq-15$ (eV)$^{-1}$. In addition, a significant enhancement of the s factor is expected for AlPdMn QCs at higher temperatures, as it is shown in Fig. 2. The value $s(\xi_1^{\exp})=3.7$ V^{-1} (dotted line) is better than that reported for both TAGS and skutterudites at $T=550$ K. Nonetheless, we should keep in mind that our rigid band model, which does not take into account the temperature dependence of E_F, will be hardly applicable at temperatures beyond the Debye one ($\Theta_D\simeq450$ K for AlPdMn).[4] Further experimental and theoretical work is then appealing in order to fully exploit the unusual transport properties of quasicrystalline alloys in thermoelectric devices.

I warmly thank Professor K. Kimura, Professor T. M. Tritt, Dr. K. Kirihara, and Dr. A. L. Pope for sharing useful materials. I acknowledge M. V. Hernández for a critical reading of the manuscript. This work was supported by the UCM through Project No. PR3/04-12450.

*Electronic address: emaciaba@fis.ucm.es

[1] G. Jeffrey Snyder and T. S. Ursell, Phys. Rev. Lett. **91**, 148301 (2003).

[2] G. Jeffrey Snyder, Appl. Phys. Lett. **84**, 2436 (2004).

[3] G. A. Slack, *CRC Handbook of Thermoelectrics*, edited by D. M. Rowe (CRC Press, Boca Raton, FL, 1995).

[4] T. M. Tritt, A. L. Pope, M. A. Chernikov, M. Feuerbacher, S. Legault, R. Cagnon, and J. Strom-Olsen, in *Quasicrystals*, edited by J. M. Dubois, P. A. Thiel, A-P. Tsai, and K. Urban, MRS Symposia Proceedings No. 553 (Materials Research Society, Pittsburgh, 1999), p. 489.

[5] A. L. Pope, T. M. Tritt, M. A. Chernikov, and M. Feuerbacher, Appl. Phys. Lett. **75**, 1854 (1999).

[6] E. Maciá, Appl. Phys. Lett. **77**, 3045 (2000).

[7] E. Maciá, Phys. Rev. B **64**, 094206 (2001).

[8] F. Morales and R. Escudero, Bull. Am. Phys. Soc. **44**, 1 (1999).

[9] K. Kirihara and K. Kimura, J. Appl. Phys. **92**, 979 (2002).

[10] T. Nagata, K. Kirihara, and K. Kimura, J. Appl. Phys. **94**, 6560 (2003).

[11] E. Maciá, Phys. Rev. B **69**, 184202 (2004).

[12] F. S. Pierce, S. J. Poon, and B. D. Biggs, Phys. Rev. Lett. **70**, 3919 (1993); F. S. Pierce, P. A. Bancel, B. D. Biggs, Q. Guo, and S. J. Poon, Phys. Rev. B **47**, 5670 (1993).

[13] A. L. Pope, T. M. Tritt, R. Gagnon, and J. Strom-Olsen, Appl. Phys. Lett. **79**, 2345 (2001).

[14] K. Kirihara, T. Nagata, and K. Kimura, J. Alloys Compd. **342**,

469 (2002).

[15] D. A. Greenwood, Proc. Phys. Soc. London **71**, 585 (1958); R. Kubo, J. Phys. Soc. Jpn. **12**, 570 (1957).

[16] C. V. Landauro, E. Maciá, and H. Solbrig, Phys. Rev. B **67**, 184206 (2003).

[17] E. Maciá, Phys. Rev. B **66**, 174203 (2002).

[18] E. Maciá, J. Appl. Phys. **93**, 1014 (2003).

[19] C. V. Landauro and H. Solbrig, Mater. Sci. Eng., A **294–296**, 600 (2000).

[20] H. Solbrig and C. V. Landauro, Physica B **292**, 47 (2000).

[21] R. Escudero, J. C. Lasjaunias, Y. Calvayrac, and M. Boudard, J. Phys.: Condens. Matter **11**, 383 (1999).

[22] T. Klein, O. G. Symko, D. N. Davydov, and A. G. M. Jansen, Phys. Rev. Lett. **74**, 3656 (1995).

[23] D. N. Davydov, D. Mayou, C. Berger, C. Gignoux, A. Neumann, A. G. M. Jansen, and P. Wyder, Phys. Rev. Lett. **77**, 3173 (1996).

[24] X. P. Tang, E. A. Hill, S. K. Wonnell, S. J. Poon, and Y. Wu, Phys. Rev. Lett. **79**, 1070 (1997).

[25] T. Klein, O. G. Symko, D. N. Davydov, and A. G. M. Jansen, Phys. Rev. Lett. **74**, 3656 (1995); D. N. Davydov, D. Mayou, C. Berger, C. Gignoux, A. Neumann, A. G. M. Jansen, and P. Wyder, *ibid.* **77**, 3173 (1996).

[26] M. A. Chernikov, A. Bianchi, and H. R. Ott, Phys. Rev. B **51**, 153 (1995).

[27] The mean value of the low temperature data reported by J. Delahaye, C. Berger, and G. Fourcaudot, J. Phys.: Condens. Matter **15**, 8753 (2003).